JOURNAL OF THEORETICAL
AND APPLIED MECHANICS
48, 2, pp. 381-395, Warsaw 2010

RADIAL RETURN METHOD APPLIED IN THICK-WALLED CYLINDER ANALYSIS

Grzegorz Widłak
Cracow University of Technology, Institute of Machine Design, Cracow, Poland
e-mail: widlak@mech.pk.edu.pl

The radial return method for elasto-plastic constitutive equations in the special case of analysis of a thick-walled cylinder is presented. Sensitivity study concerning the integration step size was performed analytically for the specified case. This simple model was also utilized in the adjustment study of nonlinear solution strategies as a preliminary phase of FEM investigations of high pressure reactors. The robustness and step-size insensitivity of this integration method was proved and efficient solution strategies were chosen.

Key words: radial return method, rate-independent plasticity, thick-walled cylinders

1. Introduction

Application of the finite element method to nonlinear structural problems is connected with iterative calculations of nodal displacements which satisfy a set of simultaneous algebraic equations of the standard linear form. An iterative operation is performed for every load level n

$$\mathbf{K}_n^i d\boldsymbol{u}_n^i = \boldsymbol{r}_n^i \qquad\qquad \boldsymbol{r}_n^i = \boldsymbol{p}_n - \boldsymbol{f}(\boldsymbol{u}_n^i) \tag{1.1}$$

where $\mathbf{K}_n^i$ is the current stiffness matrix, while $\boldsymbol{r}_n^i$ indicates unbalance between the external load vector $\boldsymbol{p}_n$ and a vector of internal forces dependent on the current nodal displacements $\boldsymbol{u}_n^i$. Subscripts refer to the n-th load level while superscripts to the i-th equilibrium iteration occurring on a specified load level. Moreover, the small step incremental approach is essential to obtain satisfactory results when the constitutive law relating stress and strain increments is path dependent.

Selection of the solution strategy and definition of convergence criteria for the iterative process depends on specified loading conditions and material characteristics. Before FEM study of complex structures, it is good practice to perform some adjustments based on the same material models but simpler geometry and loading conditions. Another essential preparatory step is sensitivity study of the constitutive integration algorithm in which constitutive equations can be enforced in a process with different increments of some imposed displacement history.

The main field of the author's investigation is an elastic-plastic analysis of a cyclically loaded thick-walled reactor with strong stress concentrators, in which shakedown effects can occur (Zieliński and Widłak, 2007; Widłak and Zieliński, 2008). In such analysis, the size of the computational model made the respective adjustment study impossible. Therefore, a simple problem of the internally loaded cylinder with plain strain conditions has been chosen.

The problem of elastic-plastic analysis of thick-walled cylinders is well known and widely presented in fundamental plasticity texts (Życzkowski, 1981). Most of them give direct solution forms. However, these analytical solutions are based on the Hencky-Iliuszyn simple process assumptions, which are not realistic in context of significant plastic deformations in contradistinction to flow theories requiring iterative approaches. Furthermore, some assumptions present in these solutions neglect certain significant aspects for specific analyses, e.g. strain hardening during cyclic loadings. The problem of thick walled cylinder analysis using incremental plasticity can be considered as the benchmark problem for procedures used in non-linear solution strategies as well as for algorithms used in the integration of constitutive relations.

2. Elastic-plastic constitutive equations. Radial return method

The finite element procedures used in structural plasticity problems require specific integration methods for constitutive and flow equations. These methods are aimed at solving the main problem in computational plasticity, in which the deformation increment is assumed to be given, while the aim is to accurately and effectively compute the corresponding stress state. If the obtained state results in residual $(1.1)_2$ larger than the prescribed tolerance, then a new equilibrium iteration is generated, and the next increment calculated. The secondary problem, which is related to constitutive relations, is calculation of the elasto-plastic stress-strain matrix along with certain strategies as a means to finding the solution.

The radial-return method (Simo and Taylor, 1986; Hughes, 1984; Simo and Hughes, 1998) is the most widely used and effective algorithm for this purpose. When striving for benchmark objectives, it suffices to consider this algorithm with simplified plasticity models. An essential idea concerning the problem, which assumes an elastic-perfectly plastic case with the Huber-von Mises yield surface and the associated flow rule, is outlined below.

Generally, the following set of governing equations has to be satisfied (Bathe, 1995; Belytschko *et al.*, 2000)

$$\dot{\sigma}_{ij} = C^E_{ijrs}(\dot{\varepsilon}_{rs} - \dot{\varepsilon}^{pl}_{rs}) \tag{2.1}$$

in which $\dot{\sigma}_{ij}$ represents stress rates, C^E_{ijrs} are components of the elastic constitutive tensor and $\dot{\varepsilon}_{rs}$, $\dot{\varepsilon}^{pl}_{rs}$ are components of total and plastic strain rates, respectively.

The Huber-von Mises yield function can be stated in the following form

$$f = \frac{3}{2}(s_{ij} \cdot s_{ij}) - Y^2 \tag{2.2}$$

where s_{ij} are deviatoric stress components and Y denotes the yield stress. This function gives the yield condition $f = 0$, which must hold throughout the plastic response.

Assuming the active process, the plastic strain rates are given by the Prandtl-Reuss flow rule

$$\dot{\varepsilon}^{pl}_{ij} = \dot{\lambda}\frac{\partial f}{\partial \sigma_{ij}} \tag{2.3}$$

where $\dot{\lambda}$ is related to the effective plastic strain rate and the flow direction is indicated as normal to the von Mises cylinder.

Equations (2.1) and (2.3) are further reduced by enforcing the consistency condition $f = 0$, which forms a nonlinear equation on $\dot{\lambda}$ and leads to the following rate constitutive equations

$$\dot{\sigma}_{ij} = C^{ep}_{ijrs}\dot{\varepsilon}_{rs} \tag{2.4}$$

where C^{ep}_{ijrs} are components of the tensor which is often referred as a matrix of the continuum elasto-plastic tangent moduli.

In fact, in FEM computations, we have no longer continuum problems described by the previous constitutive equations, therefore, the incremental models as the return mapping algorithm are employed. In the following, an outline of this method is presented which further is illustrated in the particular case of analysis of a thick walled cylinder. Moreover, the elasto-plastic tangent operator, consistent with the radial-return algorithm, is derived in the specified case.

In the development of this algorithm, it is beneficial to present geometrical interpretation of equation (2.1). It is observed that in a plastic process the stress $\dot{\boldsymbol{\sigma}}$ is an orthogonal projection of the trial vector $\dot{\boldsymbol{\sigma}}^{tr}$ onto the tangent plane of the yield surface. This is caused by normality of the involved plastic strain rate vector $\dot{\boldsymbol{\varepsilon}}^{pl}$ (Fig. 1).

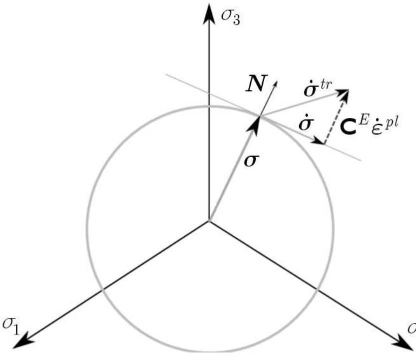

Fig. 1. Geometric interpretation of the constitutive relation for elastic-perfectly-plastic cace with the Huber-von Mises yield surface

The first task of the algorithm is to calculate the elastically induced trial stress $\boldsymbol{\sigma}_n^{tr}$ for a given strain increment $d\boldsymbol{\varepsilon}$. The trial stress is examined to confirm whether it is inside or outside the yield surface. If it falls within or on the yield surface, the process is recognized as an elastic one, and the update stress is simply equal to the trial stress

$$\boldsymbol{\sigma}_n^{tr} = \boldsymbol{\sigma}_{n-1} + \mathbf{C}^E d\boldsymbol{\varepsilon} \tag{2.5}$$

where $\mathbf{C}^E$ is an elastic constitutive matrix (see (4.1)).

If the trial stress lies outside the yield surface, it is necessary to bring it back accordingly to the consistency condition. In the radial return process, $\boldsymbol{\sigma}_n$ is defined as an intersection of the line connecting the trial stress to the center of the yield surface with this surface (Fig. 2).

The algorithm is convergent and exact in the limit when $d\boldsymbol{\varepsilon} \to \mathbf{0}$. Moreover, the algorithm is recognized as being much more accurate than more complex procedures, and works satisfactorily even for large increments resulting from a small number of the applied load steps. The sensitivity study of this phenomenon was analytically performed for the thick walled cylinder problem in Section 7, and the algorithm robustness was proved.

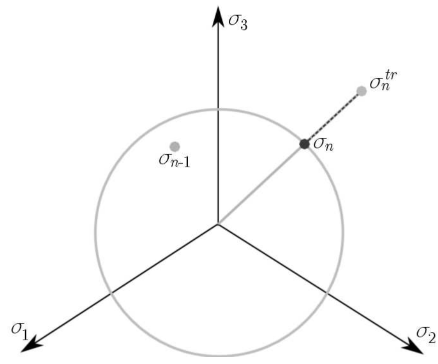

Fig. 2. Illustration of the radial-return algorithm

3. Advanced nonlinear solution strategies

To proceed further, it is worthwhile to review the role played by different solution strategies in the overall nonlinear analysis process. A chosen strategy has significant influence on the generated strain increment size and the rate of solution convergence.

In equation $(1.1)_1$, the matrix K_n^i takes on the role of a stiffness matrix in linear analysis, but now it relates small changes of load to small changes of displacements. This global stiffness matrix is computed or modified for a given deformation state, then inverted and applied to the nodal out-of-balance force vector to obtain the displacement increments. The general objective of each iteration in equation $(1.1)_1$ can be represented as out-of-balance force reduction

$$\boldsymbol{r}_n^{i+1} = \boldsymbol{p}_n - \boldsymbol{f}(\boldsymbol{u}_n^{i+1}) = \mathbf{0} \tag{3.1}$$

The form of the stiffness matrix, which is used at subsequent iterations, depends on the assumed solution method. Various schemes have been developed to solve nonlinear problems. In this section, a group of Newton methods are discussed, which are the most common algorithms used in FEM computations.

In the most often used Newton-Raphson procedure, equation (3.1) can be approximated to the first order as

$$\boldsymbol{r}_n^{i+1} \cong \boldsymbol{r}_n^i + \Big(\frac{\partial \boldsymbol{r}}{\partial \boldsymbol{u}}\Big)_n^i d\boldsymbol{u}_n^i = \mathbf{0} \tag{3.2}$$

The stiffness matrix, corresponding to the tangent direction, can be presented in this case as

$$(\mathsf{K}_T)_n^i = \Big(\frac{\partial \boldsymbol{f}}{\partial \boldsymbol{u}}\Big)_n^i = -\Big(\frac{\partial \boldsymbol{r}}{\partial \boldsymbol{u}}\Big)_n^i \tag{3.3}$$

This matrix is assembled in the actual FEM procedures using element matrices, which are determined on the basis of constitutive elasto-plastic tangent operators

$$(\mathbf{K}_T^e)_n^i = \int_e \mathbf{B}^\top (\mathbf{C}^{ep})_n^i \mathbf{B}\, dV_e \tag{3.4}$$

where $\mathbf{B}$ matrix defines relation between the strain vector and nodal displacements, and $(\mathbf{C}^{ep})_n^i$ is the constitutive matrix on the n-th step and i-th iteration defined in a tensoric form by equation (2.4) and calculated using the return mapping algorithm.

Finally, equation (3.2) can be rewritten as follows

$$(\mathbf{K}_T)_n^i d\boldsymbol{u}_n^i = \boldsymbol{r}_n^i \tag{3.5}$$

contributing to actual displacements

$$\boldsymbol{u}_n^{i+1} = \boldsymbol{u}_n^i + d\boldsymbol{u}_n^i \tag{3.6}$$

The N-R process is distinguished by very rapid convergence in which the asymptotic rate is quadratic. The main drawbacks of this process are connected with computation of the tangent stiffness matrix and factorization at each iteration.

An obvious modification of this procedure involves retention of the original tangent stiffness matrix, calculated and factorized at the first iteration to current load levels. In this case, however, the rate of convergence is much lower – linear asymptotic instead of quadratic.

Other methods eliminating the tangent stiffness formation at every iteration utilize secant directions, which can be computed taking advantage of the known previous displacement increment and out of balance force reduction on this increment. A secant slope can be used in such a way that

$$(\mathbf{K}_S)_n^{i+1} d\boldsymbol{u}_n^i = \boldsymbol{r}_n^i - \boldsymbol{r}_n^{i+1} \tag{3.7}$$

This is called the quasi-Newton equation. It does not uniquely define $(\mathbf{K}_S)_n^{i+1}$, but places a restriction on its definition. By using this approach, one may obtain convergence much more rapidly than in the modified N-R process.

Up to now, several different procedures of determining $(\mathbf{K}_S)_n^{i+1}$ have been proposed. All of them use some form of updating previously determined matrices or their inverses. For example, one of them, preserving the matrix symmetry and positive definiteness, is the BFGS (Broyden, Fletcher, Goldfarb, Shanno) update (Dennis and More, 1977). This method is effectively used with recomputation and factorization of the tangent matrix after some number of secant matrix updates, which can, however, sometimes lead to instability when a higher number of updates is involved. It will be investigated in Section 6.

The common feature of iterative techniques discussed above is the resultant displacement in the vector form $d\boldsymbol{u}_n^i$, the purpose of which is to reduce $\boldsymbol{r}_n^{i+1}$ to zero. This is not always easy to achieve in several iterations and depends on loading conditions, material characteristics and the chosen solution strategy. To get a solution which represents faster convergence, a modification of equation (3.6) can be introduced as (Crisfield, 1991)

$$\boldsymbol{u}_n^{i+1} = \boldsymbol{u}_n^i + s_n^i d\boldsymbol{u}_n^i \tag{3.8}$$

where s_n^i is a scalar search parameter. This, so called, line search technique is an important feature of most numerical techniques of optimization and can be used in a wide range of iterative solution procedures. For the simple iterative procedures outlined above, the scalar s_n^i would be set to unity. In equation (3.8), the scalar s_n^i becomes a variable, which can be determined for a scalar nonlinear system by evaluating $\boldsymbol{r}_n^{i+1}$ for various values of $\boldsymbol{u}_n^{i+1}$. For multi-degree-of-freedom systems such an approach is rather complex. It requires the introduction of a scalar parameter $S(s_n^i)$ of residual forces, which can be stored while selecting s_n^i, when

$$\boldsymbol{r}_n^{i+1} = \boldsymbol{p}_n - \boldsymbol{f}(\boldsymbol{u}_n^{i+1}) \tag{3.9}$$

has a zero component in the direction of $d\boldsymbol{u}_n^i$. This yields

$$S(s_n^i) = d\boldsymbol{u}_n^i \cdot \boldsymbol{r}_n^{i+1} = 0 \tag{3.10}$$

which is a nonlinear scalar equation for s_n^i. During one iteration several evaluation of this function should be performed. Matthies and Strang (1979) suggest accepting s_n^i if $|S(s_n^i)| < 0.5|S(0)|$.

With the line search technique, acceleration of convergence is remarkable, especially when applied to the modified Newton or quasi Newton methods. In many commercial systems, it is even enclosed into the standard N-R procedure giving significant reduction to the number of iterations (Hallquist, 2006).

4. Implicit integration algorithm for thick walled cylinders

As written previously, the cylindrical high-pressure vessels are the main interest of the author. Therefore, a thick-walled cylinder has been chosen to illustrate the problem presented earlier in general form. The plane strain state has been assumed, i.e. $\dot{\varepsilon}_z = 0$. In this case, in the plane strain conditions the system of equations (2.1) changes to

$$\begin{Bmatrix} \dot{\sigma}_r \\ \dot{\sigma}_\theta \\ \dot{\sigma}_z \end{Bmatrix} = \mathbf{C}^E \begin{Bmatrix} \dot{\varepsilon}_r - \dot{\varepsilon}_r^{pl} \\ \dot{\varepsilon}_\theta - \dot{\varepsilon}_\theta^{pl} \\ -\dot{\varepsilon}_z^{pl} \end{Bmatrix} \tag{4.1}$$

where

$$\mathbf{C}^E = \frac{2G}{1-2\nu} \begin{bmatrix} (1-\nu) & \nu & \nu \\ \nu & (1-\nu) & \nu \\ \nu & \nu & (1-\nu) \end{bmatrix} \qquad G = \frac{E}{2(1+\nu)}$$

Yield function (2.2) can be defined as

$$f = \frac{1}{2}[(\sigma_r - \sigma_\theta)^2 + (\sigma_\theta - \sigma_z)^2 + (\sigma_z - \sigma_r)^2] - Y^2 \tag{4.2}$$

where σ_r, σ_θ, σ_z are the radial, hoop, axial stress, respectively and Y is the yield stress. In the particular case, the flow rule takes the form

$$\begin{Bmatrix} \dot{\varepsilon}_r^{pl} \\ \dot{\varepsilon}_\theta^{pl} \\ \dot{\varepsilon}_z^{pl} \end{Bmatrix} = \dot{\lambda} \begin{Bmatrix} 2\sigma_r - \sigma_\theta - \sigma_z \\ 2\sigma_\theta - \sigma_r - \sigma_z \\ 2\sigma_z - \sigma_r - \sigma_\theta \end{Bmatrix} \tag{4.3}$$

where $\dot{\lambda}$ is related to the effective plastic strain rate $\dot{\varepsilon}_{eq}^{pl}$ as follows

$$\dot{\lambda} = \frac{\dot{\varepsilon}_{eq}^{pl}}{2Y} \Big[\frac{1}{\mathrm{MPa} \cdot \mathrm{s}}\Big] \tag{4.4}$$

The effective plastic strain rate is defined as

$$\dot{\varepsilon}_{eq}^{pl} = \sqrt{\frac{2}{3}[(\dot{\varepsilon}_r^{pl})^2 + (\dot{\varepsilon}_\theta^{pl})^2 + (\dot{\varepsilon}_z^{pl})^2]} \tag{4.5}$$

For the numerical implementation and compatibility with the Newton type algorithms, it is required to represent equation (4.1) in the incremental form. There are several techniques of calculation of the stress states $\boldsymbol{\sigma}_n$ located on the yield surface. Herein, a direct method corresponding to the return mapping algorithm is presented. Equations (4.1) and (4.3) can be developed to

$$\begin{Bmatrix} \sigma_r \\ \sigma_\theta \\ \sigma_z \end{Bmatrix}^{(n)} = \begin{Bmatrix} \sigma_r \\ \sigma_\theta \\ \sigma_z \end{Bmatrix}^{(n-1)} + \mathbf{C}^E \begin{Bmatrix} d\varepsilon_r - d\varepsilon_r^{pl} \\ d\varepsilon_\theta - d\varepsilon_\theta^{pl} \\ -d\varepsilon_z^{pl} \end{Bmatrix} =$$
$$= \begin{Bmatrix} \sigma_r \\ \sigma_\theta \\ \sigma_z \end{Bmatrix}^{(tr)} - \frac{d\varepsilon_{eq}^{pl}}{2Y} \mathbf{C}^E \begin{Bmatrix} 2\sigma_r - \sigma_\theta - \sigma_z \\ 2\sigma_\theta - \sigma_r - \sigma_z \\ 2\sigma_z - \sigma_r - \sigma_\theta \end{Bmatrix}^{(n)} \tag{4.6}$$

where

$$\begin{Bmatrix} \sigma_r \\ \sigma_\theta \\ \sigma_z \end{Bmatrix}^{(tr)} = \begin{Bmatrix} \sigma_r \\ \sigma_\theta \\ \sigma_z \end{Bmatrix}^{(n-1)} + \mathbf{C}^E \begin{Bmatrix} d\varepsilon_r \\ d\varepsilon_\theta \\ 0 \end{Bmatrix} \qquad d\lambda = \frac{d\varepsilon_{eq}^{pl}}{2Y}$$

were introduced.

By taking advantage of the known mean plastic strain increments ($d\varepsilon_m^{pl} = 0$), we can state equations (4.6) as

$$\begin{Bmatrix} \sigma_r \\ \sigma_\theta \\ \sigma_z \end{Bmatrix}^{(n)} = \begin{Bmatrix} \sigma_r \\ \sigma_\theta \\ \sigma_z \end{Bmatrix}^{(tr)} - 2G d\lambda \begin{Bmatrix} 2\sigma_r - \sigma_\theta - \sigma_z \\ 2\sigma_\theta - \sigma_r - \sigma_z \\ 2\sigma_z - \sigma_r - \sigma_\theta \end{Bmatrix}^{(n)} \tag{4.7}$$

In an implicit algorithm, in contradistinction to the explicit algorithm, the right hand side of equations (4.7) is computed in the final state, which is indicated by superscript n. Using (4.7), we can calculate $\boldsymbol{\sigma}_n$ as

$$\begin{aligned} \sigma_r^{(n)} &= \frac{2G d\lambda(\sigma_r^{(tr)} + \sigma_\theta^{(tr)} + \sigma_z^{(tr)}) + \sigma_r^{(tr)}}{6G d\lambda + 1} \\ \sigma_\theta^{(n)} &= \frac{2G d\lambda(\sigma_r^{(tr)} + \sigma_\theta^{(tr)} + \sigma_z^{(tr)}) + \sigma_\theta^{(tr)}}{6G d\lambda + 1} \\ \sigma_z^{(n)} &= \frac{2G d\lambda(\sigma_r^{(tr)} + \sigma_\theta^{(tr)} + \sigma_z^{(tr)}) + \sigma_z^{(tr)}}{6G d\lambda + 1} \end{aligned} \tag{4.8}$$

These values must satisfy the yield condition. By introducing them into (4.2), we obtain a nonlinear equation in $d\lambda$ which is dependent on $d\varepsilon_{eq}^{pl}$

$$\frac{(\sigma_r^{(tr)} - \sigma_\theta^{(tr)})^2 + (\sigma_\theta^{(tr)} - \sigma_z^{(tr)})^2 + (\sigma_z^{(tr)} - \sigma_r^{(tr)})^2}{2(6G d\lambda + 1)^2} - Y^2 = 0 \tag{4.9}$$

Once $d\lambda$ is determined, all terms of the vector $\boldsymbol{\sigma}_n$ can be calculated by substituting specified values into (4.8).

5. Elastic-plastic tangent stiffness matrix for plane strain

When the presented algorithm is included into the Newton type solution strategies, the tangent stiffness matrix is needed. This can be obtained employing equation (3.4) which uses the tangent stress-strain operators. It is well proved (Simo and Taylor, 1985; Ristinmaa, 1994; Hughes and Belytschko, 2008) that significant loss in the rate of convergence occurs when the elasto-plastic continuum tangent matrix is used in place of the tangent consistently derived from the integration algorithm. The consistent operator is defined as

$$\mathbf{C}_n^{ep} = \frac{\partial \boldsymbol{\sigma}(\boldsymbol{\sigma}_{n-1}, \boldsymbol{\varepsilon}_{n-1}, \varepsilon^{pl}_{eq_{n-1}}, \boldsymbol{\varepsilon} - \boldsymbol{\varepsilon}_{n-1})}{\partial \boldsymbol{\varepsilon}}\Big|_{\boldsymbol{\varepsilon}=\boldsymbol{\varepsilon}_n} \tag{5.1}$$

and can be obtained in practice by differentiation of stresses (4.8) with respect to time and application of condition (4.9). This enables us to find the rate of $d\varepsilon^{pl}_{eq}$ as a function of the deformation rate. The elasto-plastic matrix finally takes the following form

$$\begin{aligned}\mathbf{C}_n^{ep} &= \frac{2G}{\Big(6G\frac{d\varepsilon^{pl}_{eq}}{2Y}+1\Big)(1-2\nu)}\begin{bmatrix} \mathcal{A}+(1-\nu) & \mathcal{A}+\nu \\ \mathcal{A}+\nu & \mathcal{A}+(1-\nu) \\ \mathcal{A}+\nu & \mathcal{A}+\nu \end{bmatrix} + \\ &-\frac{1}{2Y}\Big(1-\frac{d\varepsilon^{pl}_{eq}}{Y}\frac{\partial Y}{\partial(d\varepsilon^{pl}_{eq})}\Big)\frac{1}{\frac{\partial f}{\partial(d\varepsilon^{pl}_{eq})}}\begin{bmatrix} d_1d_1 & d_1d_2 \\ d_2d_1 & d_2d_2 \\ d_3d_1 & d_3d_2 \end{bmatrix}\end{aligned} \tag{5.2}$$

where subsequently

$$\mathcal{A} = \frac{Gd\varepsilon^{pl}_{eq}}{Y}(1+\nu) \qquad d_1 = \frac{2G(2\sigma_r-\sigma_\theta-\sigma_z)}{6G\frac{d\varepsilon^{pl}_{eq}}{2Y}+1}$$

$$d_2 = \frac{2G(2\sigma_\theta-\sigma_r-\sigma_z)}{6G\frac{d\varepsilon^{pl}_{eq}}{2Y}+1} \qquad d_3 = \frac{2G(2\sigma_z-\sigma_r-\sigma_\theta)}{6G\frac{d\varepsilon^{pl}_{eq}}{2Y}+1}$$

The above matrix is of the same kind as the one presented by Simo and Taylor (1985), which in contradistinction to the continuum matrix used in (2.4) preserves quadratic rate of convergence in conjunction with the full Newton method.

6. Adjustment study of the solution strategy

The problem of thick-walled cylinder analysis in the elasto-plastic range is considered as the benchmark test for procedures used in the iterative nonlinear solution as well as for the radial return algorithm. The dimensions and internal pressure of the investigated cylinder correspond to geometry and loading conditions of actual high-pressure reactors, i.e. internal radius $a = 150$ mm, external radius $b = 300$ mm and pressure $p = 150$ MPa. An elastic-perfectly plastic material with the yield stress $Y = 200$ MPa was assumed for the tests.

The nonlinear iterative strategies presented in the previous section were employed by the author in the solution of the problem listed above, which was comparatively solved with modern FE codes – Ansys and LS-Dyna. The full Newton method and quasi Newton with the BFGS updates method proved respectively, the fastest convergence rate. However, the second one was more effective because it needed calculation and factorization of the tangent stiffness matrix only at the first iteration of every load increment. The most effective solution procedure was the BFGS method in conjunction with line search technique. The displacement increment was scaled using the line search as long as the scalar parameter of residual forces $S(s_n^i)$ satisfied the condition $|S(s_n^i)| < 0.5|S(0)|$. This condition was sufficient in obtaining convergence in 4 iterations without matrix recalculations (Fig. 3). The rate of convergence was almost quadratic, characteristic for the full Newton method, and the computational time was proved to be three times shorter. Therefore, the quasi Newton method with the BFGS updates was chosen in the detailed investigations of the thick walled reactors with stress concentrators.

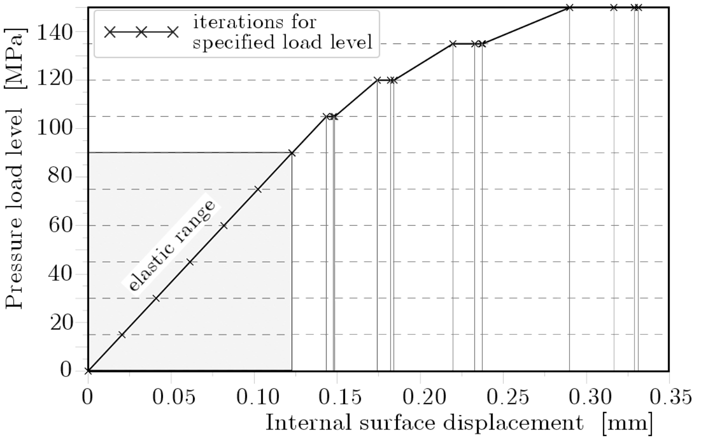

Fig. 3. Iterations in the quasi Newton method with the line search

There are some ways of determining the nonlinear solution convergence. The most popular are criteria based on specified norms and certain threshold values. The procedure continues to calculate equilibrium iterations until the convergence tolerance is satisfied. Different values of tolerances are suggested for various problems in the commercial nonlinear FE systems. The influence of the convergence criteria on the calculated hoop stress is shown in Fig. 4. Other stress components present a very similar course, therefore, the author resigned from presenting these plots. It suffices to use $\varepsilon_d = 1\%$ relative tolerance for the displacement and residual force norms. The energy relative convergence tolerance must be set to $\varepsilon_c = 0.1\%$ in order to obtain accurate results. This last value is approximately one order smaller than this suggested by nonlinear FE systems (Hallquist, 2006). It is best to use a double-check on the convergence, e.g. simultaneous monitoring of the displacement and energy norms. This last approach was utilized in the investigation of the reactor.

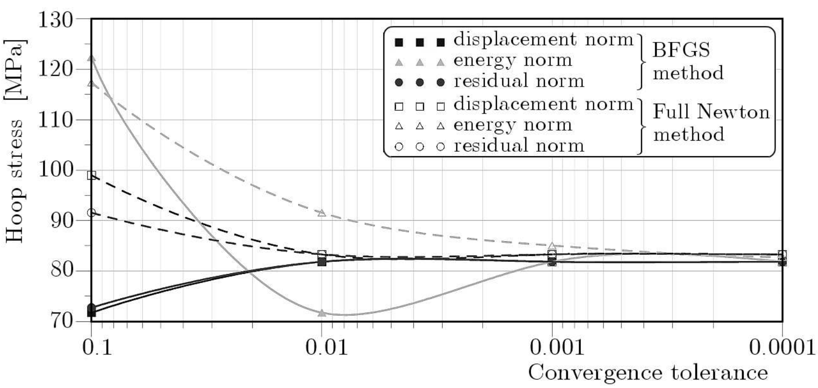

Fig. 4. Convergent hoop stresses for various tolerance norms (LS-Dyna)

7. Radial return algorithm study

The presented return-mapping integration algorithm, in conjunction with the quasi Newton solution strategy, is stable for a wide range of nonlinear problems that involve small deformations. The accuracy considerations are limited to investigations of the load increment size. In the examination of this algorithm, certain deformations were applied, from which the trial stress state was analytically calculated. With the use of Eq. (4.9), $d\lambda$ was determined and $\boldsymbol{\sigma}_n$ components were calculated from (4.8). The solution for a large number of 10 000 steps was treated as the reference deformation history. This was further divided into different numbers of increments and used in the study of the algorithm convergence.

Even in the one-step calculations, a very good accuracy was achieved (Fig. 5). The stress components differed approximately by 1 MPa from the reference level. The inaccuracy associated with the choice of convergence criteria had a greater influence on the obtained results in the overall solution process (see Fig. 4). Hence, this investigation proved robustness and step-size insensitivity of the radial return algorithm.

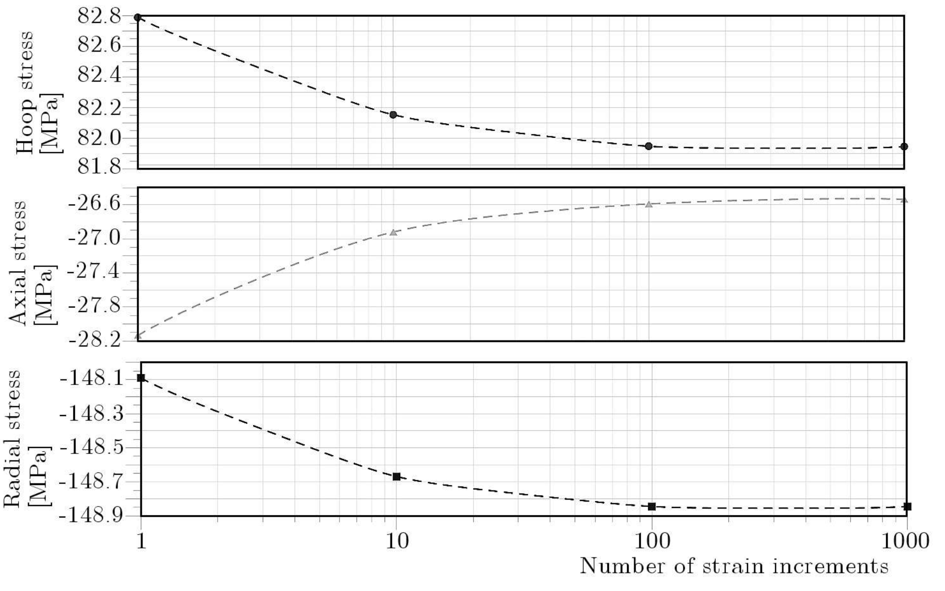

Fig. 5. Sensitivity study of the radial return algorithm used in an analytical way (Eqs. (4.8)-(4.9))

8. Conclusions

The radial return algorithm was described and illustrated with the special case of analysis of the thick-walled cylinder in the plane strain conditions. This simple model was also utilized in the adjustment study of nonlinear solution strategies as a preliminary phase of FEM investigations of high pressure reactors. The return mapping algorithm, applied in the Huber-von Mises associated plasticity, is a robust and step-size insensitive integration method.

A closer scrutiny is suggested for a choice of the solution strategy and setting of parameters of the nonlinear solution convergence, because they mainly influence the efficiency and accuracy of the nonlinear solution process.

Acknowledgement

I wish to thank Professor Andrzej P. Zieliński, PhD. Eng. for his essential guidance and for revising my manuscript.

This work was supported by Polish Ministry of Science and Higher Education – grant No. 1353/T02/2007/32.

References

1. Bathe K.J., 1995, *Finite Element Procedures*, Prentice-Hall
2. Belytschko T., Liu W.K., Morgan B., 2000, *Nonlinear Finite Elements for Continua and Structures*, J. Wiley & Sons, New York
3. Crisfield M.A., 1991, *Non-linear Finite Element Analysis of Solids and Structures, Vol. 1: Essentials*, J. Wiley & Sons, New York
4. Dennis J.E., More J., 1977, Quasi-Newton methods, motivation and theory, *SIAM Review*, **19**, 1, 46-89
5. Hallquist J., 2006, *LS-Dyna Theory Manual*, Livermore Software Technology Corporation
6. Hughes T., 1984, Numerical implementation of constitutive models: rate-independent deviatoric plasticity, *Theoretical Foundation for Large-Scale Computations for Nonlinear Material Behaviour*, Martinus Nijhoff Publishers, The Netherlands
7. Hughes T., Belytschko T., 2008, *A Course of Nonlinear Finite Element Analysis*, Paris
8. Jetteur P., 1986, Implicit integration algorithm for elastoplasticity in plane stress analysis, *Engineering Computations*, **3**, 3, 251-253
9. Matthies H., Strang G., 1979, The solution of nonlinear finite element equations, *International Journal for Numerical Methods in Engineering*, **14**, 11, 1613-1626
10. Ristinmaa M., 1994, Consistent stiffness matrix in FE calculations of elasto-plastic bodies, *Computers and Structures*, **53**, 1, 99-103
11. Simo J.C., Taylor R.L., 1985, Consistent tangent operators for rate-independent elastoplasticity, *Computer Methods in Applied Mechanics and Engineering*, **48**, 101-118

12. SIMO J.C., TAYLOR R.L., 1986, A return mapping algorithms for plane stress elastoplasticity, *International Journal for Numerical Methods in Engineering*, **22**, 3, 649-670

13. SIMO J.C., HUGHES T., 1998, *Computational Inelasticity*, Springer-Verlag, New York

14. WIDŁAK G., ZIELIŃSKI A.P., 2008, Local shakedown analysis of reactors subject to pressure and thermal loads, *Proc. 8th World Congress on Computational Mechanics*

15. ZIELIŃSKI A.P., WIDŁAK G., 2007, Local shakedown analysis in regions of holes in high-pressure vessels, *Proc. IX International Conference on Computational Plasticity*

16. ŻYCZKOWSKI M., 1981, *Combined Loadings in the Theory of Plasticity*, PWN-Polish Scientific Publishers, Warsaw

Metoda rzutowania powrotnego w analizie stanu naprężeń cylindra grubościennego

Streszczenie

W pracy zaprezentowano metodę rzutowania powrotnego dla szczególnego przypadku analizy sprężysto-plastycznej cylindra grubościennego. Wykorzystując analityczne zależności, zbadano dokładność tej metody dla różnych wielkości przyrostów odkształceń. Zagadnienie analizy sprężysto-plastycznej cylindra grubościennego zostało również wykorzystane do oceny metod nieliniowego rozwiązywania zagadnień MES, które następnie będą użyte w badaniu reaktorów wysokociśnieniowych. W pracy wykazano dużą dokładność analizowanego algorytmu.

Manuscript received April 20, 2009; accepted for print September 24, 2009